

MEASUREMENT OF MARS ROTATIONAL VARIATIONS VIA EARTH-BASED RADIO TRACKING OF MARS LANDERS

Robert D. Kahn* , William F. Folkner* ,
Robert A. Preston' , Charles D. Edwards, Jr.‡

The INTERMARSNET mission currently under study by the European Space Agency (ESA) and NASA involves the deployment of four Mars landers which will perform seismologic, rotational, magnetic and meteorological measurements to infer the internal structure of the planet, its magnetic properties, and atmospheric circulation and weather patterns. The measurements of Mars' rotational variations are to be conducted via weekly Earth-based radio tracking observations of the lander network over one Martian year (687 days). Two-way carrier phase measurements between an Earth antenna and each of the landers will enable precise monitoring of the planet's orientation and length-of-day variations, allowing details of Mars' internal structure and global surface/atmosphere interactions to be determined for the first time. An analysis has been performed to investigate the accuracy with which key physical parameters of Mars can be determined using the Earth-based radio tracking measurements. Acquisition of such measurements over one Martian year should enable determination of Mars' polar moment of inertia to 0.1 %, providing a strong constraint on radial density profiles (and hence on the iron content of the core and mantle) and on long-term variations of the obliquity and climate of Mars. Variations in Mars length of day and polar motion should also be detectable, and will yield information on the seasonal cycling of CO₂ between the atmosphere and the surface.

INTRODUCTION

The INTERMARSNET mission currently jointly under study by the European Space Agency (ESA) and NASA involves the deployment of a network of four Mars landers¹. Seismologic data acquired from the lander network will serve as a sensitive probe into the internal structure of the planet by monitoring the propagation of seismic waves through Mars' interior. Earth-based tracking of the lander network provides complementary information by measuring the planet's rotational irregularities which are caused principally by the torque exerted on Mars by the Sun, but which may also have components arising from the dynamics of a fluid core or surface/atmosphere interactions. Accurate monitoring of variations in Mars' orientation over a large fraction of a Martian year enables extremely accurate estimation of the polar principal moment of inertia. The Mars pole precesses about 7.5 arcsec per year, equivalent to 50 m displacement at the planet's surface. Determination of the moment of inertia, and hence the rate of precession, to within 0.1% would impose

* Member Technical Staff, Tracking Systems and Applications Section, Jet Propulsion Laboratory

† Technical Group Supervisor, Tracking Systems and Applications Section, Jet Propulsion Laboratory

‡ DSN Technology and Science Office, Jet Propulsion Laboratory

significant constraints on models for the composition of the planet's interior² Knowledge of the moment of inertia is also a key to understanding long term changes in the obliquity and resultant climate variations. Accurate measurement of the semiannual nutation of the pole would determine the size of the Mars liquid core to an accuracy of 100 km (Ref. 3). Earth-based tracking of the lander network is also sensitive to polar motion (movement of the crust relative to the spin axis) and variations in Mars' length-of-day. Mars is expected to have semiannual and annual-period length-of-day variations of amplitude 20 ms (equivalent to a 5 m change in position at the planet's surface) due to the seasonal sublimation and refreezing of the Mars polar ice caps⁴, and may have detectable polar motion resulting from asymmetry in polar ice cap deposition. An accurate record of these effects over a Martian year would lead to a better understanding of the seasonal cycling of CO₂ between the atmosphere and the planet's surface.

An earlier study⁵ showed that decimeter-level determination of Mars precession, nutation and length-of-day variation is possible via simultaneous Earth-based tracking of a net work of three Mars landers (a decimeter at the surface of Mars corresponds to a rotation of 6 mas). In that analysis, the orientation of Mars was modeled as comprising linear terms to account for precession, and annual and semi-annual period sinusoidal nutation terms for each angular component of the pole position. In the current analysis, rather than directly estimating the amplitudes of various nutation terms, many of which are highly correlated, we employ a simple physical model for the Mars interior and estimate key physical parameters which affect the precession and nutation amplitudes.

The next section contains a brief description of the information content of differenced two-way carrier phase measurements from Earth-based tracking, of two or more Mars landers. The following sections describe the physical model used to describe the rotation of Mars and the measurement accuracy of lander-differenced carrier phase data. Finally, a covariance analysis is presented and the results are discussed.

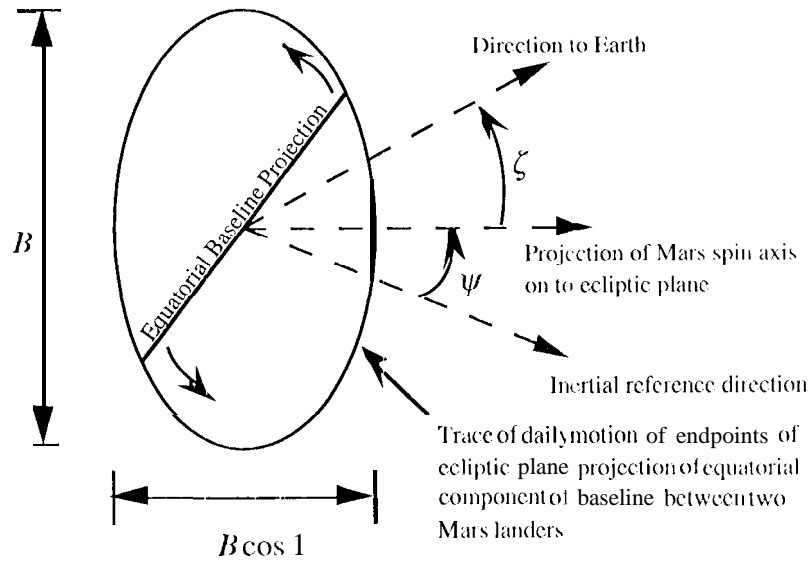
MEASUREMENT INFORMATION CONTENT

The data type being considered in this analysis is differenced two-way carrier phase. An Earth antenna uplinks a carrier signal to two or more Mars landers, each of which coherently transponds the carrier signal. The returning signals are phase-locked at the Earth antenna, and the signal phase from each pair of landers is differenced. The differenced phase measurement is insensitive to Earth rotation, Earth-Mars relative motion, and fluctuations in delay due to the Earth and Mars tropospheres and ionospheres; the signature in the lander-differenced carrier phase data arises from changes in the relative range between the landers and the Earth antenna as the landers rotate about the Mars spin axis. Over a Martian day, the projection on to the ecliptic plane of the equatorial component of the lander-lander baseline traces out an ellipse with major axis B and minor axis $B \cos(I)$, where B is the equatorial component of the baseline and I is the obliquity of Mars (the inclination of the Mars equator relative to the ecliptic plane). The geometry is depicted in Figure 1.

If the Earth-Mars direction is parallel to the projection of the Mars rotation axis on to the ecliptic plane, then the lander-differenced range, $\Delta r(t)$, is of the form

$$\Delta r(t) = B \cos(I) \cos(\omega_M t + \phi_0)$$

where I is the obliquity of Mars (the inclination of the Mars equator relative to the Mars orbit), and ω_M is the rotation rate of Mars. If the Earth-Mars direction is orthogonal to the



B = Length of equatorial component of baseline between two Mars landers

I = Angle between Mars spin axis and ecliptic north pole

Figure 1 Geometry of Mars lander motion projected into the ecliptic plane (viewed from North ecliptic pole)

projection of the Mars rotation axis on to the ecliptic plane, then the lander-differenced range is of the form

$$\Delta r''(t) = B \cos(\omega_M t + \phi_0)$$

In general, if Earth lies an angle ζ from the projection of the Mars spin axis on to the ecliptic plane, the lander-differenced range takes the form:

$$\Delta r(t) = \sin \zeta [B \sin(\omega_M t + \phi_0)] + \cos \zeta [B \cos I \cos(\omega_M t + \phi_0)] \quad (1)$$

Equation (1) shows that the differenced range signature is sensitive to the obliquity, I , and the ecliptic longitude of the Mars pole, ψ (a small perturbation of ψ produces an equivalent perturbation in the angle ζ).

In order to gain additional insight into the information content of two-way lander-differenced range it is instructive to consider a simple case where the Mars network consists of 4 landers --- an East-West (EW) baseline formed by two landers on the equator, and a North-South (NS) baseline consisting of two landers which lie on a common longitude and are equidistant from the equator. Both the EW and NS baselines are of length B . Conventionally, for the Earth, rotational variations are broken into five component angles, two describing the direction of the angular momentum vector in inertial space, one describing the angle of rotation about the moment of inertia vector, and two describing the orientation of the surface with respect to the moment of inertia vector (polar motion). This decomposition is employed so that slowly varying angles may be used to describe the rotational variations of the angular momentum vector.

Sensitivity to I and ψ

If the nominal value of I is inaccurate by an amount δI , then the differenced range obtained from the East-West lander pair will exhibit a residual signature of

$$\delta(\Delta r(t)) = -\delta I \cos \zeta [B \sin I \sin(\omega_M t + \phi_0)] \quad (2)$$

If the Earth-Mars direction is perpendicular to the projection of Mars' spin axis on to the ecliptic plane (i.e. $\zeta = 90^\circ$), then differenced range measurements are completely insensitive to variations in I . On the other hand, when $\zeta = 0^\circ$, the amplitude of the residual signature is $\delta I B \sin I$. If the EW baseline is 1000 km, [hen since $I \approx 25^\circ$, the amplitude of the signature is about 400 km $\times \delta I$. Thus, for example, an error of 50 mas in the obliquity would produce a diurnal differenced-range signature of amplitude 10 cm.

If the nominal value of ψ is inaccurate by an amount $\delta\psi$, then the nominal value of ζ is also inaccurate by an amount $\delta\psi$. The differenced range obtained from the EW base] inc will exhibit a residual signature of

$$\delta(\Delta r(t)) = \delta\psi B \{ \cos \zeta \sin(\omega_M t + \phi_0) - \sin \zeta \cos I \cos(\omega_M t + \phi) \} \quad (3)$$

Thus, depending on the value of ζ at the time of the measurement, the amplitude of the residual signature is between $B\delta\psi$ and $B\delta\psi \cos(I) \approx 0.9 B\delta\psi$. For a 1000 km lander baseline, an error of 50 mas in ψ would produce a diurnal differenced-range signature of amplitude 22 to 24 cm.

Differenced range measurements from the NS lander baseline are completely insensitive to perturbations of I and ψ since the NS baseline has zero equatorial projection.

Sensitivity to Polar Motion

Polar motion refers to a small rotation of the planet's crust figure axis with respect to the moment of inertia, effectively moving the pole of figure. A crustal rotation of $\delta\theta$ of the EW baseline about an axis parallel to the baseline would not change its equatorial projection and would therefore not alter the differenced range signature. A rotation of $\delta\theta$ about the axis which lies in the equatorial plane and bisects the EW baseline would change the equatorial projection of the EW baseline by an amount

$$\delta(\Delta r(t)) = B(1 - \cos(\delta\theta)) \approx B(\delta\theta)^2/2 \quad (4)$$

Thus, depending on the value of ζ at the time of the measurement, the residual differenced range signature would have amplitude between $B(\delta\theta)^2/2$ and $0.411 B(\delta\theta)^2/2$. If the baseline length is 1000 km, then a deviation of 50 mas would produce a diurnal differenced-range signature with amplitude on the order of 10^{-7} cm — much too small to be detected from lander-differenced range measurements.

A rotation of $\delta\theta$ about either the X or Y figure axes would increase the equatorial projection of NS from zero to $B \sin(\delta\theta) \approx \delta\theta B$. If the baseline length is 1000 km, then a deviation of 50 mas in polar motion would produce a diurnal differenced-range signature with amplitude 24 cm.

Table 1

**SENSITIVITY OF LANDER-DIFFERENCED CARRIER PHASE MEASUREMENTS
TO PERTURBATIONS OF MARS ORIENTATION PARAMETERS**

	Amplitude, in cm, of lander-differenced range signature from SO mas perturbation of Mars orientation parameter	
Parameter	1000 km NS Baseline	1000 km EW Baseline
I	0	0-10 [†]
ψ	0	22-24 [†]
X_p	24	0
Y_p	24	0
ϕ	0	10-24 [†]

[†]Amplitude depends on value of ζ at time of observation (see Figure 1 and Eq.(1))

- Note: 1) 50 mas perturbation of Mars orientation is equivalent to 82 cm of displacement at the planet's surface
2) Sensitivities are directly proportional to baseline length

Sensitivity to Length of Day

For the EW baseline, a perturbation of ϕ of the rotational orientation of Mars about its spin axis results in a residual differenced-range signature of

$$\delta(\Delta r(t)) = \delta\phi \{ \sin \zeta [B \cos(\omega_M t + \phi_0)] - \cos \zeta [B \cos I \sin(\omega_M t + \phi_0)] \} \quad (5)$$

Thus, depending on the value of ζ at the time of the measurement, the amplitude of the residual signature is between $B\delta\phi$ and $B\delta\phi \cos(I) \approx 0.4 B\delta\phi$. Since the equatorial component of the NS baseline is zero, it is not sensitive to perturbations of the rotational orientation of Mars about its spin axis.

The sensitivity of differenced-range data to variations in the orientation angles is summarized in Table 1. Lander-differenced carrier phase measurements acquired from the EW and NS baselines are sensitive to complementary components of Mars orientation. While the NS baseline is sensitive to the two components of polar motion, X_p and Y_p , it is completely insensitive to variations in I , ψ , and ϕ . In contrast, the EW baseline is sensitive to the latter parameters, but not to polar motion. Thus, in order to recover information about all of the orientation parameters it is important that data be acquired from baselines with components in both the NS and EW directions.

MARS ROTATION MODEL.

Our model for the rotation of Mars is based on the work of Reasenber and King⁶. The transformation from a Mars crust-fixed coordinate, x , to the standard IME 2000 inertial vector r is given by

$$r = R_z(-N)R_x(-I)R_z(-\psi)R_x(-I)R_z(-\phi)R_y(X_p)R_x(Y_p) x$$

where $R_i(\theta)$ represents a counter-clockwise rotation about axis i through an angle θ , e.g.

$$R_x(\theta) = \begin{pmatrix} 1 & 0 & 0 \\ 0 & \cos \theta & \sin \theta \\ 0 & -\sin \theta & \cos \theta \end{pmatrix}$$

X , and Y , are the crust-fixed coordinates of Mars' spin axis; ϕ is the rotation about the spin axis; I is the inclination of the (instantaneous) Mars equator to the (fixed) Mars mean orbit plane of J2000; ψ is the longitude of the Mars spin axis in the mean Mars orbital plane of J2000 measured with respect to the intersection of Mars' mean orbit and Earth's mean equator of J2000; N and J transform between the inertial Mars-mean-orbit system and the Earth-mean-equator system of J2000 with J the inclination of Mars mean orbital plane relative to Earth's mean equator and N the angle between Earth's equinox and the intersection of Mars' mean orbit and Earth's mean equator of J2000.

For a rigid Mars, the changes in the direction of Mars' spin axis in inertial space due to torques from the Sun and other solar system bodies are described by series expansions of the angles I and ψ :

$$I(t) = I_0 + \sum_1^{\infty} I_m \cos(\alpha_m t + \theta_m) \quad (6)$$

$$\psi(t) = \psi_0 + \dot{\psi} t + \sum_1^{\infty} \psi_m \sin(\alpha_m t + \theta_m)$$

The trigonometric arguments in Eqs. (6) involve multiples of the mean anomaly of Mars, M , and the angle $q = 2\Omega + 2\omega - 2\psi$, where Ω is the longitude of the Mars orbit ascending node with respect to the Earth mean ecliptic, measured from the Earth's equinox, and ω is the argument of periapsis. The rate of change of M is the mean motion, n , while the rate of change of q is negligible. The amplitude coefficients I_m , ψ_m and $\dot{\psi}$ are functions of Mars' orbital elements and principal moments of inertia. The dominant uncertainty in the motion of Mars' spin axis is due to uncertainty in the polar principal moment of inertia, C ; the amplitude coefficients are proportional to the quantity $(C - A)/C$, where A is the moment of inertia about an axis in the plane perpendicular to the spin axis (we assume axial symmetry about the spin axis). The quantity $C - A$ is well determined from measurements of the J_2 component of the gravity field⁷. Only a small number of terms is needed to describe the motion of Mars' pole at the milliarcsecond level; we use the terms through $m = 9$.

To model the fluid core within the rigid mantle, the periodic motion of the spin axis is expressed in prograde and retrograde terms, r_m and p_m :

$$I_m \cos(\alpha_m t + \theta_m) + i \sin(I_0) \psi_m \sin(\alpha_m t + \theta_m) = r_m e^{-i(\alpha_m t + \theta_m)} + p_m e^{i(\alpha_m t + \theta_m)}$$

The nominal prograde and retrograde are modified by the fluid core according to⁸

$$r'_m = r_m \left(1 + \frac{\alpha_m}{\alpha_m - \sigma_0} \right) \quad (7)$$

$$p'_m = p_m \left(1 + \frac{\alpha_m}{\alpha_m - \sigma_0} \right),$$

where σ_0 is the free core nutation rate, and the parameter F is ratio of the core moment of inertia to the moment of inertia of the solid body. Since the coefficients p_m and r_m in Eqs. (7) are linear combinations of I_m and ψ_m , they are proportional to $1/\omega$.

In the covariance analysis we use the transformations from Mars crs(-fixed coordinates given above and solve for corrections to the coefficients C , F , and σ_0 with nominal values 0.365, 0.070, and 1.5 deg/day respectively. In addition, for each observation session, we solve for an independent value of rotation variation about the pole, ϕ , and X and Y polar motion since we expect these to vary randomly due to interactions between the planet's surface and atmosphere.

MEASUREMENT ACCURACY

The signal transmitted by the Earth tracking station is acquired by the Mars landers and coherently transponded back to Earth. Between the time it arrives at the spacecraft antenna and is retransmitted, the signal undergoes a variety of phase and group delays induced by filters and other components in the spacecraft telecommunications subsystem. These delays vary with time and with the changing environmental conditions at the landing site, particularly the temperature. Diurnal temperature variations at the landing site will give rise to diurnal variations in the transponder delays; the resulting signature in the lander-differenced phase may be confused with diurnal signatures resulting from errors in the nominal Mars orientation parameters. The extent to which lander transponder delay variations interfere with the parameter estimation depends strongly on the magnitude of the delay variations. This dependence is investigated by considering a variety of transponder delay stabilities, ranging from 40 to 600 picoseconds per day. As a baseline we use a stability of 75 pscc which is characteristic of the Cassini transponder over the temperature range expected to be experienced by the electronics on the surface of Mars⁹. Within the covariance analysis, each lander's transponder delay is modeled as a random walk parameter growing in uncertainty by 75 pscc per day. To test the validity of this model, a simulated 4 hour arc of lander-differenced data was generated with variations in Mars rotation angles and diurnal signatures for the delay on each lander transponder. The diurnal signatures had 75 pscc amplitude and phase proportional to the elevation of the sun. The lander transponder delays were modeled as random walks and the amplitude and phase of the diurnal signature were estimated along with the rotation variations. The resulting estimates and 1-sigma uncertainties of the rotation parameters were consistent with the values inserted for the simulation.

Radio signals propagating through interplanetary space undergo significant phase variations arising from electron density fluctuations in the solar wind along the signal path. These fluctuations become increasingly pronounced as the Sun-Ihu-th-Probe (SEP) angle decreases and the signal traverses denser regions of solar plasma. The contribution of the solar plasma to lander-differenced phase error is computed using a statistical model for the phase fluctuations derived from thousands of hours of Viking S and X Band radio-tracking measurements¹⁰. The plasma-induced phase noise on lander-differenced phase measurements is not white phase noise, but because of limitations inherent in the filtering software, it is simpler to model it as white and compensate for this mismodeling by scaling the noise level appropriately. If the Mars landers are separated by 1000 km, and the Sun-Earth-Mars angle is 25°, then the two-way lander differenced phase measurement error over 5 minutes is estimated to be 1.8 mm if the Earth-lander link is at a 2.3 GHz radio frequency (S-band). This level of measurement error is small enough that the rotation determination is dominated by the lander transponder stability. (The phase error would be even smaller at the 8.4 GHz X-band frequency). A detailed discussion of the solar plasma phase error is presented in the Appendix.

A number of other effects corrupt the lander-differenced phase measurements at a level smaller than the solar plasma noise. There is white noise in measuring the two-way carrier phase depending on the received signal to noise ratio. However if the landers transmit an equivalent isotropic radiated power (EIRP) of 1 W to a DSN 70 m antenna, then the phase measurement error is smaller than the solar plasma noise. Uncalibrated phase dispersion (non-linear phase response) in the Earth station instrumentation also introduces an error in the lander-differenced phase measurement. The uncalibrated phase dispersion at S-Band is about 0.18 mm (Ref. 11).

The lander-differenced phase measurements undergo phase fluctuations induced by signal propagation through the tropospheres and ionospheres of Earth and Mars. If the landers are separated by 1000 km on Mars, then their maximum angular separation as viewed from Earth is 13 μ rad, when the Earth-Mars distance is at its minimum (0.5 AU). As a result, Earth media-induced phase fluctuations on the signals cancel nearly completely. For example, if the zenith delay through the Earth's troposphere is calibrated to 4 cm, the error in lander-differenced phase is less than 0.1 mm for elevations greater than 5°, assuming a cosecant tropospheric delay mapping function. Similarly, lander-differenced phase fluctuations induced by the Earth's ionosphere are vanishingly small, assuming typical zenith total electron content calibration to 5×10^{16} el/m². (Zenith TEC is the path integral of the electron density through the ionosphere, in the zenith direction.) Because the angular separation of the Mars landers as viewed from Earth is so small, errors in the location of the Earth antenna, and Earth orientation errors cancel nearly perfectly when the phase from the two Mars landers is differenced.

For Mars landers separated by hundreds or thousands of kilometers, the effects of the Martian troposphere and ionosphere on the carrier signals are largely independent. However, the neutral atmosphere and ionosphere of Mars are much more tenuous than those of Earth; these delays change gradually during a tracking pass as the elevations of the signal ray paths change. We assume that the total zenith troposphere delay of 4 cm can be calibrated to 10% using *in-situ* atmospheric pressure measurements, and that the total zenith TEC is 1×10^{16} el/m (Ref. 12), equivalent to 8 cm of delay on an S-Band signal. The change in the tropospheric and ionospheric delays resulting from the changing elevation of the signal path over 5 minutes is a fraction of a millimeter.

Imperfect knowledge of the relative position of Earth and Mars introduces an error on the lander-differenced phase data which varies over the Earth-Mars synodic period. The JPL ephemeris DE234¹³ exhibits uncertainties of order 10 nrad in the apparent angular position of Mars as viewed from Earth, due primarily to uncertainties in the relative inclinations of the Earth and Mars orbit planes.

COVARIANCE ANALYSIS

A covariance analysis was performed to determine the ability to estimate Mars orientation and physical parameters using lander-differenced phase measurements from a triad of landers. The landers were oriented in an isosceles right-triangle with one 1000 km baseline oriented East-West and the other 1000 km baseline oriented North-South. Four hours of lander-differenced phase measurements from both baselines were simulated during once-weekly tracking passes beginning on 2-January 2004, and continuing for one Mars year. The differenced phase measurements were scheduled at one of the 70 m DSN antennas. The lander network was chosen arbitrarily; any similar arrangement with baselines about 1000 km long and significant North-south and East-West baselines should give comparable results.

The covariance analysis assumptions are summarized in Table 2. Estimated parameters modeled as constants include the angular coordinates of the Mars pole position l and ψ , the Mars polar moment of inertia C , the ratio of the core moment of inertia to the solid body moment of inertia, F , the free core nutation rate, σ_0 , a length of day correction, ϕ , Mars X Polar Motion, X_p , Mars Y Polar Motion, Y_p , and the lander locations. All parameters except ϕ and polar motion are modeled as constants over the two-year data arc. The parameters ϕ , X_p , and Y_p are estimated independently for each pass.

The differenced phase data are weighted at 1.8 mm to account for measurement errors arising from the solar plasma, thermal noise, and instrumental phase dispersion. In the initial analysis, lander transponder delays are modeled as random walks with variance growing by $(75 \text{ psec})^2$ per day.

Table 2
COVARIANCE ANALYSIS ASSUMPTIONS

Mars Lander Locations

	<u>Latitude (deg)</u>	<u>Longitude (deg)</u>
Lander 1	2	2
Lander 2	2	22
Lander 3	22	2

Data Schedule

Once-weekly 4-hour tracking passes at a single Earth antenna
Jan. 2, 2004 to Nov. 27, 2005.

Two-way lander-differenced phase data weighted at 1.8 mm (S-rein integration)

Estimated Parameters

	<u>Nominal Value</u>	<u>A Priori Uncertainty</u>
Polar moment of inertia, C	0.365	0.5
Moment of inertia ratio, F	0.07	0.5
Free core nutation rate, σ_0	1.5 deg/day	1.0 deg/day
Mars obliquity at J2000, I_0	25.19202 deg	0.5 deg
Mars pole longitude at J2000, ψ_0	-98.02561 deg	0.5 deg
Mars length of day correction, ϕ^\dagger	0 deg	1 deg
Mars X polar motion, X_p^\dagger	0 deg	1 deg
Mars Y polar motion, Y_p^\dagger	0 deg	1 deg
Lander locations		1000 km/component
Lander transponder delays ^{††}		0.1 s

† Estimated parameters modeled as constants over the two year data arc except:

† estimated independently for each weekly pass

†† estimated as random walk whose variance grows by $(75 \text{ psec})^2$ per day

Considered (Unadjusted) Parameters

	<u>Uncertainty</u>
Mars zenith troposphere delay	4111111
Mars zenith TEC	$1 \times 10^{16} \text{ el/m}^2$
Earth station locations	3 cm/component
Earth Polar Motion	1 mas/component
Earth UT1	70 μsec
Mars-Earth ephemerides	Covariance from JPL J234 ($\approx 10 \text{ nrad}$)

To address errors arising from mismodeling of the Mars and Earth media effects, the Earth and Mars ephemerides, and Earth orientation and the Earth station's location, a consider analysis was performed. "Considered" parameters are not estimated; rather the formal parameter uncertainties calculated by the least-squares analysis are increased by an amount corresponding to the sensitivity of the parameters to uncertainties in the considered parameters. The Mars zenith troposphere delay, and zenith TEC are assigned uncertainties of 4 mm and 1×10^{-6} el/m², respectively. The Earth and Mars ephemeris elements are assigned a covariance derived from the J111, DE234 ephemeris. Earth station location uncertainties are assumed to be 3 cm/component, Earth polar motion uncertainty is 1 mas/component, and uncertainty in Earth UT1 is 70 μ sec.

The results of the covariance analysis are summarized in Table 3. Mars' polar moment of inertia is determined to 0.1 % of its nominal value; the uncertainty on the estimate of the moment of inertia ratio, F , is 0.011. The free core nutation rate, σ_0 , can be estimated to 0.02 deg/day which corresponds to uncertainty of ± 3 days in the free core nutation period, assuming a nominal period of 240 days. Because Mars polar motion and rotation about its spin axis are estimated independently for each of the 98 weekly passes over the two year period, Table 5 reports the range of uncertainties obtained for each of these parameters. All lie between 4 and 24 mas (corresponding to 7-40 cm at the planet's surface). Finally, the angular coordinates of the Mars spin axis at J2000, I_0 and ψ_0 , can be measured to 2 and 43 mas, respectively. For all of the parameters, the formal uncertainty dominates; the most significant consider parameter is the Mars troposphere.

The covariance analysis used a data weight of 1.8 mm for S-rein lander-differenced phase points. As was discussed earlier, the lander-differenced phase measurement error is dominated by signal transmission through the solar plasma. The calculated error was 1.8 mm for Sun-Earth-Mars (SEM) angle of 25° , but solar plasma-induced phase fluctuations on the received signals depend strongly on the SEM angle, which is greater than 25° during most of the Earth-Mars synodic period. It turns out, however, that the covariance analysis results change little if the data noise is dynamically decreased to account for the changing SEM angle. In fact, uniformly decreasing the measurement noise by an order of magnitude changes the errors of the Mars parameter estimates by only 5 percent.

Table 3
COVARIANCE ANALYSIS RESULTS
(Four hour data arcs, 75 psec transponder delay stability)

Parameter	Formal Uncertainty	----- Consider Errors* -----			RSS
		Mars Trop	Mars Ion	Ephemeris	
C	3.7×10^{-4}	2.4×10^{-4}	0.5×10^{-4}	0.5×10^{-4}	4.5×10^{-4}
F	0.011	0.001	0.000	0.001	0.011
σ_0 (deg/day)	0.019	0.005	0.001	0.000	0.020
I_0 (mas)	1.9	0.7	0.1	0.1	2.0
ψ_0 (mas)	36.4	22.3	5.0	4.0	43.2
ϕ^{\dagger} (mas)	8-23	5-10	1-3	0-1	10-24
X_p^{\dagger} (mas)	5-7	4-5	0-1	0	7.9
Y_p^{\dagger} (mas)	3-6	1-3	0-1	0	4.7

*Errors due to J111 media, Earth station location uncertainty, and Earth orientation uncertainty are vanishingly small and therefore not included in this table.

[†]Range of values obtained from 98 independent weekly climates performed over 2 year period.

The accuracy of the parameter estimates is limited not by the data weight but rather by the lander transponder delay stability. To investigate this dependence, additional analyses were performed in which the lander transponder delay was varied between 40 and 300 psec. The results are summarized in Figure 2, in which the total errors (RSS of the formal and consider errors) are shown for each parameter. The accuracy of the parameter estimates depends almost linearly on the transponder delay stability for all of the parameters.

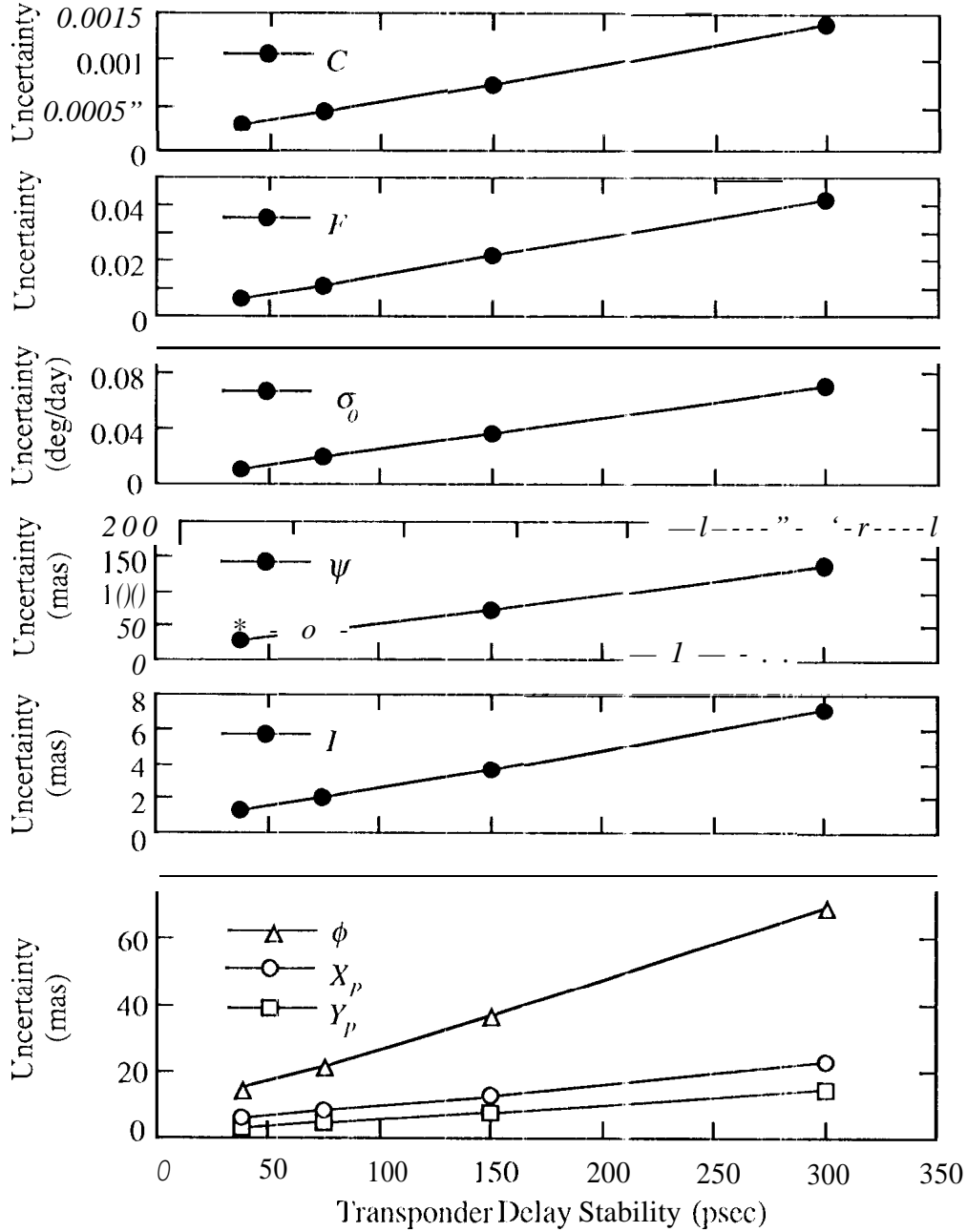


Figure 2 Covariance analysis results as a function of transponder delay stability

We have also considered the impact of using data arcs which are shorter than 4 hours. Figure 3 illustrates the change in parameter estimate uncertainties as the data arc length is varied between 1 and 4 hours. For each of these cases we have assumed transponder delay stability of 75 psec. The most significant benefit of increased data arc length is accrued as the tracking passes are increased from 1 to 2-3 hours. In this regime, the accuracy of the parameter estimates increases much faster than the square root of the number of measurements because the longer data arcs capture a larger fraction of the diurnal sinusoids' signatures in the data. The marginal benefit in increasing from 3 to 4 hours is less pronounced, though still somewhat better than the square root of the number of measurements.

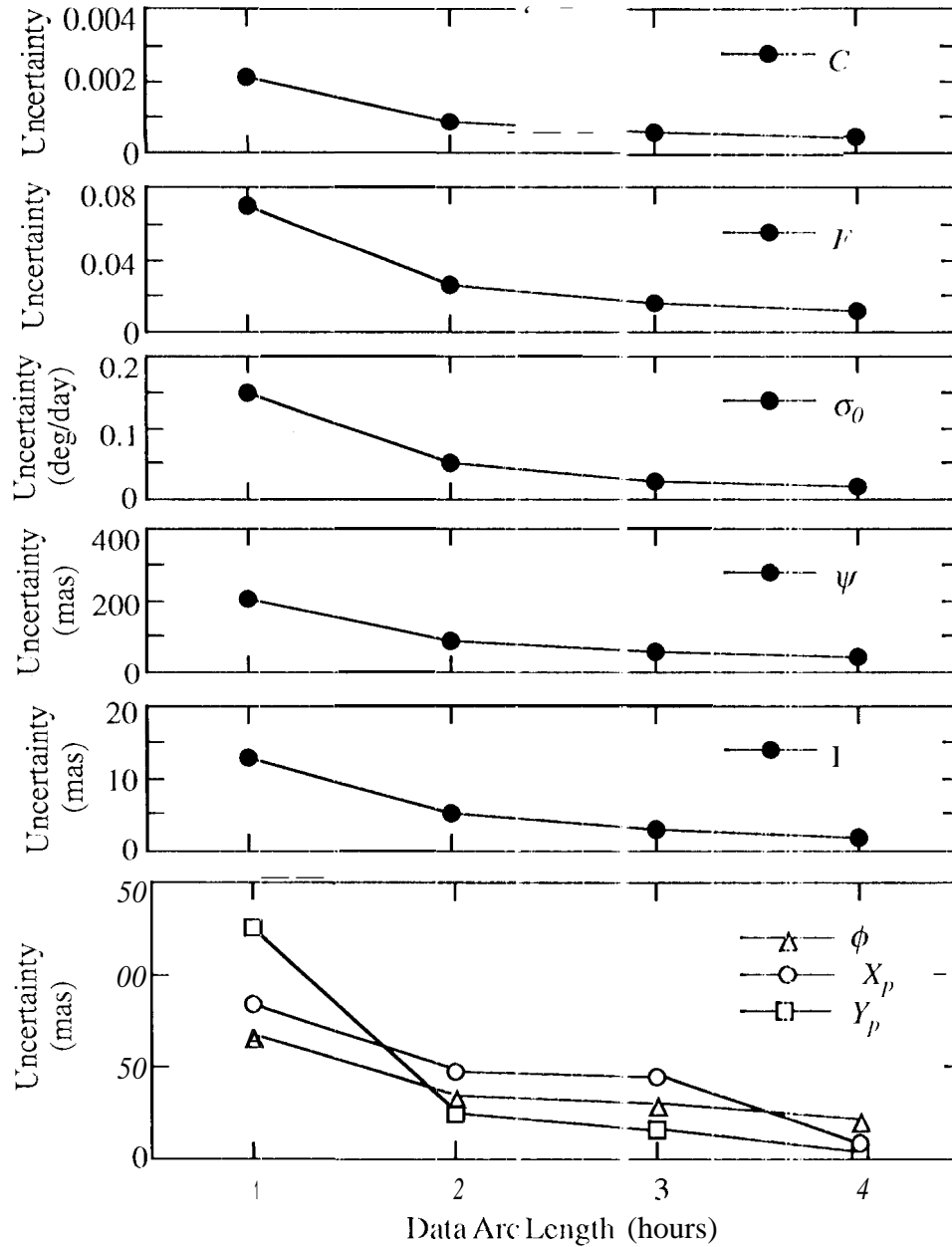


Figure 3 Covariance analysis results as a function of data arc length

CONCLUSION

The tracking strategy described in this study offers a straightforward scheme for measuring rotational variations of Mars --- weekly simultaneous 2-way tracking of a carrier phase signal between an Earth antenna and a network of Mars landers. The landers are arranged so that pairs of them define 1000 km baselines in the North-South and the East-West directions. For best results, the weekly tracking passes should be several hours in duration. Using this tracking strategy, the orientation of Mars can be monitored with unprecedented accuracy.

The ability to recover Mars orientation information from lander-differenced carrier phase depends strongly on the diurnal thermal delay stability of the lander transponders, as well as the length of the data arcs. The dependence on transponder delay stability is practically linear in the regime of stabilities ranging from 40-300 psec. The parameter estimates improve significantly as the data arcs are lengthened to 3 or 4 hours. Assuming lander transponder delay stability of 75 psec, 4 hour data arcs allow estimation of Mars' polar moment of inertia to 0.1%, i.e. the 50 m annual procession of Mars can be measured with 5 cm accuracy. This is accurate enough to provide a strong constraint on radial density profiles for the planet's interior, in particular enabling bounds to be set on the iron content of the core and mantle. Furthermore, such accurate knowledge of the polar moment of inertia would provide constraints on the long term variations in Mars' obliquity and climate. We have also shown that Mars' polar motion and length-of-day variability can be measured to the 4-24 mas (7-40 cm) level. This is sufficiently accurate to enable detection of predicted length-of-day variations and polar motions arising from the seasonal melting and re-freezing of the CO₂ ice caps at the planet's poles.

ACKNOWLEDGMENT

The research described in this paper was carried out by the Jet Propulsion Laboratory, California Institute of Technology, under a contract with the National Aeronautics and Space Administration.

REFERENCES

1. ESA M3 Selection Process: Presentation of Assessment Study Results, SC I(94)9, May 1994.
2. Bills, B. G., "Geodetic Constraints on the Composition of Mars," *J. Geophys. Res.* vol. 95, No. B9, pp. 14131-14136, Aug 30, 1990.
3. Hilton, J. L., "The Motion of Mars' Pole: I. Rigid Body Precession and Nutation. II. The Effect of an Elastic Mantle and a Liquid Core," *Ph.D. Dissertation*, US Naval Observatory, Washington, DC 1991.
4. Cazenave, A. and G. Balmino, "Meteorological Effects of the Seasonal Variations of the Rotation of Mars," *Geophys. Res. Letters* 8245-248, 1981.
5. Edwards, C. D., R. D. Kahn, W. M. Folkner, and R. A. Preston, "Mars Planetary Geodesy Using Earth-Based Observations of Mars Landers," *Proceedings of the AIAA/AAS Astrodynamics Conference*, Hilton Head SC, August 10-12, 1992.
6. Reasenberg, R. D. and R. W. King, "The Rotation of Mars", *J. Geophys. Res.*, Vol 84, No. B11, pp 6231-40, October 10, 1979.
7. Smith, D. E. et al., "An Improved Gravity Model for Mars: Goddard Mars Model 1," *J. Geophys. Res.*, Vol 98, No. E 11, pp. 20871-20889, Nov 25, 1993.
8. Yoder, C., Private communication, 1994.

9. Mysoor, N. R., J. D. Perret, and A. W. Kennode, "Design Concepts and Performance of NASA X-band (71 62 MHz/8415 MHz) Transponder for Deep-Space Spacecraft Applications," *TDA Progress Report 42-104*, Jet Propulsion Laboratory, Pasadena, California, pp. 247-256, February 15, 1991.
10. Woo, R. and J. Armstrong, "Spacecraft Radio Scattering Observations of the Power Spectrum of Electron Density Fluctuations in the Solar Wind," *J. Geophys. Res.*, Vol. 84, No. A12, pp. 7288-96, Dec 1, 1979.
11. Edwards, C., "Mark III VC Phase Response", JPL Interoffice Memorandum (Internal Document), February 20, 1989.
12. Zhang, M. H. G., J. G. Lunmann, A. J. Kliore, and J. Kim, "A Post-Pioneer Venus Reassessment of the Martian Dayside Ionosphere as Observed by Radio Occultation Methods," *J. Geophys. Res.*, Vol. 95, No. 69, pp 14829-39, August 30, 1990.
13. Standish, E. M., "The JPL Planetary anti Lunar Ephemerides DE234/LE235," JPL Interoffice Memorandum 314.6-1348 (Internal Document), October 8, 1991.
14. Kahn, R. D. and J. S. Border, "Precise Interferometric Tracking of Spacecraft at Low Sun-Earth-Probe Angles," *Paper A/AA-88-0572*, AIAA 26th Aerospace Sciences Meeting, Reno, Nevada, January 11-14, 1988.

APPENDIX

To model solar plasma-induced fluctuations on radio signals transmitted by interplanetary spacecraft, the plasma is imagined to be confined to a thin screen passing through the center of the sun and perpendicular to the line connecting the spacecraft and the earth. This construction is valid only when the Sun-Earth-Mars angle is less than 90° , but in this development we are concerned with the effect of the plasma when it is most significant — at small Sun-Earth-Mars angles. A random function, $\phi(x)$, represents the phase fluctuation induced on a radio signal as it penetrates the plasma screen at a distance x from the center of the sun. Then the quantity $\phi(b+x) - \phi(x)$ represents the differential phase fluctuation induced on two signals which are separated by a distance b when passing through the plasma screen. Since Mars is 1.5 times farther from the Sun than is Earth, the distance b is always less than half the distance between the two landers; here we will use $b = 500''$ km.

To determine the plasma-induced phase error on radio measurements, the spatial structure function of phase, $D(b)$, is computed. The structure function of phase is defined as: $D(b) \equiv \langle (\phi(b+x) - \phi(x))^2 \rangle$. Here, brackets denote ensemble average. $D(b)$ may be viewed as representing the phase variance of a differenced phase measurement. The power spectrum of electron density fluctuations, which has been determined experimentally¹⁰ can be used to calculate a formula for $D(b)$ (Ref. 14):

$$D(b) = \frac{2.5 \times 10^{14} c}{(f_{RF})^3} \times (b/v_{sw})^{1.65} \times (\sin(SEP))^{-2.45} \text{ m}^2$$

In this expression, f_{RF} is the signal radio frequency in Hz, SEP is the Sun-Earth-Mars angle, c is the speed of light, and v_{sw} is the velocity of the solar wind (typically 400 knl/sec).

Knowledge of the structure function enables calculation of the temporal correlations between plasma-induced errors on radio measurements. First note that because of the dynamics of the solar wind, the plasma-induced phase fluctuation, ϕ , is actually a function of both space and time, $\phi = \phi(x, t)$. If however, it is assumed that the plasma turbulence consists of fixed structures which maintain their shape as they travel radially outward from the sun at velocity v_{sw} , then ϕ may be written as a function of a single variable, $\bar{\phi}(x, t) = \phi(x - v_{sw}t)$.

Let $\Delta\Phi(b, T_i) \equiv \bar{\phi}(b+x, t_i) - \bar{\phi}(x, t_i)$ and $\Delta\Phi(b, T_j) \equiv \bar{\phi}(b+x, t_j) - \bar{\phi}(x, t_j)$ be the station-differenced phase at earth receive times T_i and T_j , along a baseline whose projection onto the plasma screen has length b . Here, $t_i = T_i - \{\text{light travel time from plasma screen to earth}\}$, and $t_j = T_j - \{\text{light travel time from plasma screen to earth}\}$.

The temporal covariance is computed as

$$\begin{aligned} \langle \Delta\Phi(b, T_i) \Delta\Phi(b, T_j) \rangle &= \langle (\bar{\phi}(b+x, t_i) - \bar{\phi}(x, t_i)) (\bar{\phi}(b+x, t_j) - \bar{\phi}(x, t_j)) \rangle \\ &= \langle \bar{\phi}(b+x, t_i) \bar{\phi}(b+x, t_j) \rangle - \langle \bar{\phi}(b+x, t_i) \bar{\phi}(x, t_j) \rangle \\ &\quad - \langle \bar{\phi}(x, t_i) \bar{\phi}(b+x, t_j) \rangle + \langle \bar{\phi}(x, t_i) \bar{\phi}(x, t_j) \rangle \end{aligned}$$

Assuming ϕ is stationary,

$$\langle \bar{\phi}(x, t) \bar{\phi}(y, t') \rangle = \langle \phi(x - v_{sw}t) \phi(y - v_{sw}t') \rangle = \langle \phi(x - y - v_{sw}(t - t')) \phi(0) \rangle$$

and

$$b(p) = \langle (\phi(p+x) - \phi(x))^2 \rangle = 2 \{ \langle \phi^2 \rangle - \langle \phi \rangle^2 \}.$$

Applying the above two equations yields:

$$\langle \Delta \phi(b, T_i) \Delta \phi(b, T_j) \rangle = 1/2 D(b - v_{sw}(t_j - t_i)) + 1/2 D(b + v_{sw}(t_j - t_i)) - D(v_{sw}(t_j - t_i))$$

This expression allows the computation of a covariance matrix for an arc of measurements. However, in our parameter estimation software, we weight the lander-differenced phase points as uncorrelated white noise. We need to estimate the best white phase noise level to use so that the uncertainties in estimated model parameters reported by our program are no better than the uncertainties implied by the true solar plasma covariance.

The model parameters we estimate impose a signature on the singly-differenced phase data with a period given by Mars' rotation rate. For a single observing pass, we consider the matrix equation

$$z = Ax + v$$

where z_i is the value of the measurements, a_i are the model parameters to be estimated, $A_{i,j}$ are the partial derivatives of the measurement with respect to the model parameters, and v_i is the measurement misc. The estimated covariance on the model parameters is given by

$$\langle x_i x_j \rangle = (A^T W A)^{-1}$$

where A^T is the transpose of the partials matrix and W is the weighting matrix. The optimal least-squares estimate and covariance is given by choosing a weighting matrix that is the inverse of the actual measurement noise covariance: $W_{op} = (V)^{-1}$. If we use a different weighting matrix, the corresponding actual covariance can be computed by

$$\langle x_i x_j \rangle = (A^T W A)^{-1} A^T W \langle v_k v_l \rangle W A (A^T W A)^{-1} \quad (A1)$$

This expression for the actual covariance is independent of the scale of the weighting matrix, so we can choose the scale of the weighting matrix so that the computed covariance reported by the least-squares parameter estimation program, $A^T W A$, matches the actual covariance as closely as possible.

For this study, we considered a four-hour pass of singly differenced data taken at 1-second intervals and estimated three parameters; a phase bias and the amplitudes of $\sin(\omega t)$ and $\cos(\omega t)$ to estimate an arbitrary sinusoidal signature with ω the angular rotation rate of Mars. We find, for a frequency of 2.3 GHz and SEP of 25° that using a white measurement noise of 2.3 cm gives a computed covariance $(A^T W A)^{-1}$ for the estimated parameters that is slightly (<5%) larger than the actual covariance obtained from Eq. (A1). The actual covariance is about 10% larger than the optimal covariance, $(A^T W_{op} A)^{-1}$, indicating that we pay a 10% penalty for not having the capability to use the true measurement covariance in forming the parameter estimates. For our simulations we

have compressed our data to 5-minute points, for which the 1-way white-phase noise would be 1.3 mm. The corresponding noise level for two-way measurements is 1.8 mm. We have used this noise level for all SEP angles so we are being fairly conservative in our data weights.